Rigid Element Model for the dynamic behaviour of masonry façades in building aggregates

DANIELE BARALDI
Department of Architecture
Università Iuav di Venezia
Terese, Dorsoduro 2206, 30123, Venezia
ITALY

Abstract: - In this short contribution, an existing discrete/rigid block/element model, able to study the in- and out-of-plane behaviour of masonry walls with regular texture, is extended and adapted for performing out-of-plane modal analysis of large-scale masonry façades taken from building aggregates. A generalisation of the existing model is proposed in order to discretise large masonry façades by means of quadrilateral rigid elements, without significantly increasing the computational effort of modal analyses with respect to more detailed models having rigid blocks. An efficient tool is also proposed for the definition of rigid element geometric characteristics and the definition of contacts between the elements, starting from a drawing exchange format file. After the evaluation of the dynamic behaviour of a simple case study represented by a small building façade, a more complex existing case study is considered for obtaining an acceptable model calibration by comparing out-of-plane modal analysis results with on-site vibrational measurements.

Key-Words: - masonry façades, building aggregates, modal analysis, rigid block model, out-of-plane behaviour, structural identification

Received: March 23, 2026. Revised: May 7, 2026. Accepted: June 13, 2026. Published: November 10, 2026.

1 Introduction

In Europe and especially in southern Europe regions, historical town centres are characterised by monuments and minor architecture that are essential parts of the built cultural heritage. Historical centres are mostly made of UnReinforced Masonry (URM) buildings, often built in aggregate, which are extremely vulnerable in case of seismic actions; see, for instance, the surveys made after the latest strong earthquakes in Italy [1], [2], [3], [4], [5].

Accurate approaches for studying the structural behaviour of masonry buildings in town centres are the analytical ones or direct methods. The former ones are based on analytic [6], [7], [8] or numerical models. The latter ones can be based on equivalent frame modelling [9], [10], finite element modelling (FEM) [11], [12], and limit analysis approaches [13]. These models often require a large computational effort and, consequently, are applied to small building aggregates. However, in the case of complex masonry building aggregates, analyses can primarily focus on out-of-plane behaviour, typical of façades not well connected to other structural elements of the building. In this field, simplified numerical models may be adopted by subdividing the structure into rigid elements [14] or macro-elements [15], [16]. Moreover, different analysis types may be performed, such as limit analysis or incremental/pushover analysis. For instance, an overview of the methods for modelling masonry structures may be found in [17], and a deep literature review related to masonry out-of-plane behaviour and to existing numerical models has been proposed in [18].

In this short contribution, an existing discrete/rigid block/element model is proposed for performing out-of-plane modal analysis of masonry building façades, alone or in a building aggregate. The work is based on the original discrete model proposed in [19], where the in-plane and out-of-plane elastic behaviour of masonry walls with running bond texture was investigated. That model was successfully extended to the field of out-of-plane modal analysis of masonry panels with regular texture by adopting a matrix approach [20], even in the case of random or quasi-periodic masonry texture [21]. Here, the modal analysis approach is extended and adapted to the case of large-scale masonry façades typical of building aggregates. In this case, rigid block discretisation of the facade does not account for the actual masonry texture, but it considers quadrilateral, namely square or rectangular, rigid elements larger than single blocks, in order to reduce the computational effort of the analyses with respect to those accounting for the actual masonry texture. For this purpose, an efficient

tool is proposed that is able to acquire element geometric characteristics from a digital drawing exchange format file and to automatically determine interface position, length, and topology. The novelty of the approach is then given by the generalisation of an existing discrete/rigid block/element model for the analysis of large façades taken from single buildings or building aggregates, also by varying the level of façade discretisation, namely from a fine one close to single-block modelling, to a coarse one close to macro-element (piers, spandrels) modelling. The approach allows reducing the overall number of degrees of freedom (DOFs) of the model with respect to standard FEM approaches.

Several numerical tests are then performed to evaluate the effectiveness of the proposed approach. On one hand, a simple masonry façade with openings [22] is taken into consideration, and modal analysis results obtained with an accurate rigid block model considering the actual masonry texture are compared with those obtained with coarser models having large quadrilateral elements. On the other hand, a more complex existing case study is chosen. A quite large façade taken from the complex masonry building aggregate of 'Certosa di Padula', located in Salerno, Italy, is modelled with the proposed rigid element model. Modal analysis results are compared with existing numerical results and an on-site experimental campaign dedicated to the dynamic identification of the façade [23].

2 Rigid element model

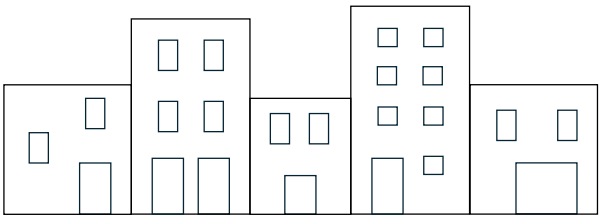


Fig. 1: Sequence of façades in a building aggregate
Source: created by the author.

This work focuses on façades of masonry building aggregates lying on the same vertical plane, by neglecting potential small geometric differences between façade portions due to varying masonry wall thickness and orientation, both in vertical direction and along the different façades of each building of the aggregate (Figure 1). Then, for describing the proposed model and approach, a single masonry building façade in plane stress state is taken into consideration (Figure 2). A global 3D coordinate system $OX_1X_2X_3$ is assumed, with OX_1X_2 denoting the façade mid-plane, and X_3 representing out-of-plane direction.

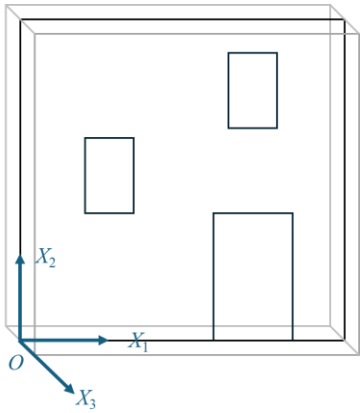


Fig. 2: Generic building façade
Source: created by the author.

2.1 Discretization

A rigid element model is defined by subdividing the façade into quadrilateral, or, better, square or rectangular, elements. Then, interfaces between the elements turn out to be horizontal and vertical only (Figure 3). It is worth noting that the discretisation in rigid elements may follow the specific structural and architectural aspects of the façades, such as openings, slab levels, and roof levels. Furthermore, discretisation can also consider the history of the individual buildings in the aggregate and their construction phases. For these reasons, façade discretisation may not necessarily be characterised by aligned elements and, subsequently, may not be characterised by aligned vertical and horizontal interfaces between the elements.

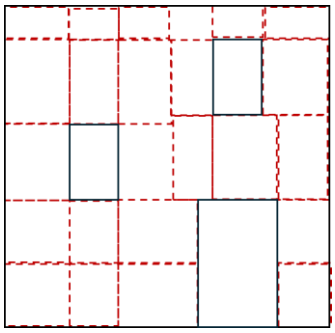


Fig. 3: Generic building façade (from Figure 2) subdivided into rectangular elements
Source: created by the author.

2.1.1 Recognition of elements and determination of interfaces

The proposed tool for element and interface recognition and definition starts from a drawing in the digital Drawing eXchange Format (DXF) containing rectangular elements or polylines in two dimensions

(2D), representing the discretisation of the façade. A fast tool for recognising and ordering all the elements and automatically determining all the interfaces between the elements is created. The main steps followed by the tool are:

- recognition of all the quadrilateral elements and determination of their area and centre coordinates, also by sorting element vertices counterclockwise;
- element reordering (since the original order is generally given by the drawing order chosen by the user) from the bottom-left corner to the top-right one of the façade;
- determination of interfaces between elements by searching for common edges or edge portions. For each interface, geometric parameters are defined (centre coordinates, length), together with their topology (rigid elements connected);
- interface reordering and cleaning.

It is worth mentioning that the step dedicated to interface determination adopts a simplified version of the contact detection algorithms often used by Discrete Element Model (DEM) codes [24]. In detail, potential adjacent elements with respect to the one considered are searched among the elements having a limited distance, equal to at least 1.5 or 2 times the maximum size of the element. Other element and interface geometric information, such as depth along the X_3 axis and interface thickness, are manually added, since they are not contained in the initial drawing.

2.2 Kinematics and equilibrium

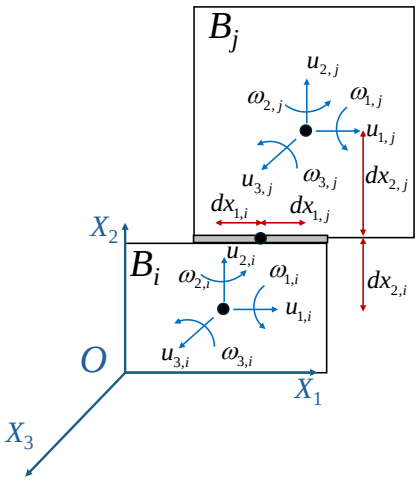


Fig. 4: Degrees of freedom of two adjacent blocks in 3D and relative distances between blocks and interface centres

Source: created by the author

Due to the hypothesis of rigid elements, the displacements of the generic i-th element are represented by three translations $u_{\alpha,i}$ of the element centre and three rigid rotations $\omega_{\alpha,i}$ of the element with respect to the axes of the coordinate system (Figure 4), with $\alpha = 1, 2, 3$ [20].

$$\mathbf{q}_i = [u_{1,i}\ u_{2,i}\ u_{3,i}\ \omega_{1,i}\ \omega_{2,i}\ \omega_{3,i}]^T \quad (1)$$

Rigid element hypothesis also allows defining the relative displacements between two generic elements connected by an interface:

$$\mathbf{d}_{i,j} = [d_{1,ij}\ d_{2,ij}\ d_{3,ij}\ \delta_{1,ij}\ \delta_{2,ij}\ \delta_{3,ij}]^T \quad (2)$$

which depend on the relative distances between each element centre and the interface centre (Figure 4). For instance, interface relative displacements are related to block relative translations and rotations:

$$\begin{aligned} d_{1,ij} &= u_{1,\mathrm{j}} - u_{1,\mathrm{i}} + dx_{2,j}\omega_{3,j} + dx_{2,\mathrm{i}}\omega_{3,i} \\ d_{2,ij} &= u_{2,j} - u_{3,i} - (dx_{1,j}\omega_{3,j} + dx_{1,\mathrm{i}}\omega_{3,i}) \\ d_{3,ij} &= u_{3,j} - u_{3,i} + (dx_{1,j}\omega_{2,j} + dx_{1,\mathrm{i}}\omega_{2,i}) + \\ &-(dx_{2,j}\omega_{1,j} + dx_{2,\mathrm{i}}\omega_{1,\mathrm{i}}) \end{aligned} \quad (3)$$

whereas interface relative rotations are only related to block rotations:

$$\delta_\alpha = \omega_{\alpha,j} - \omega_{\alpha,i} \quad (4)$$

with $\alpha = 1, 2, 3$.

The above relationships (Eq. 3) and (Eq. 4) can be written in vector and matrix form as follows:

$$\mathbf{d}_{i,j} = \mathbf{H}_{i,j} \begin{bmatrix} \mathbf{q}_i \\ \mathbf{q}_j \end{bmatrix} \quad (5)$$

$$\mathbf{H}_{i,j} = \begin{bmatrix} -\mathbf{I} & \mathbf{D}_i & \mathbf{I} & \mathbf{D}_j \\ \mathbf{0} & -\mathbf{I} & \mathbf{0} & \mathbf{I} \end{bmatrix} \quad (6)$$

$$\mathbf{D}_{(i,j)} = \begin{bmatrix} 0 & 0 & dx_2 \\ 0 & 0 & -dx_1 \\ -dx_2 & dx_1 & 0 \end{bmatrix}_{(i,j)} \quad (7)$$

where $\mathbf{H}_{ij}$ can be defined as the compatibility matrix of the interface, which relates the displacements of two adjacent blocks to the interface relative displacements. Such a matrix is frequently used with limit analysis approaches for masonry modelled by rigid elements [22].

Interface actions linearly depend on relative displacements by means of a stiffness matrix collecting normal, shear, bending, and torsional stiffness of the generic interface, depending on interface geometric characteristics and on local normal and shear stiffness (k_n, k_s) multiplied by a parameter β_{ij} accounting for the rigid element discretisation:

$$\mathbf{f}_{i,j} = \bar{\mathbf{K}}_{i,j}\,\mathbf{d}_{i,j} = (\mathbf{K}_{i,j}\mathbf{A}_{i,j})\mathbf{d}_{i,j} \quad (8)$$

$$\mathbf{K}_{i,j} = \beta_{ij}\,\mathrm{diag}\{k_s\ k_n\ k_s\ k_n\ k_s\ k_n\}_{i,j} \quad (9)$$

$$\mathbf{A}_{i,j} = \text{diag}\{A\ A\ A\ I_1\ I_2\ I_3\}_{i,j} \quad (10)$$

where A is the interface area, and I represents the second moment of inertia of the interface with respect to the three axes of the local coordinate system (parallel to the global ones).

It is worth mentioning that in this case the interface often does not represent a real interface or joint between blocks. Then, interface elastic parameters do not necessarily depend on micro-scale characteristics such as block stiffness or mortar joint stiffness, as happened with the original rigid block model, for instance [19], [20]:

$$k_n = E/e, \quad k_s = E/[2(1+\nu)]/e \quad (11)$$

where E and ν are the interface (namely mortar) elastic modulus and Poisson's ratio, respectively, and e is the interface thickness.

Here, interface elastic parameters are related to meso-scale characteristics such as overall masonry stiffness, depending, for instance, on block texture and masonry constituents' elastic properties. For this purpose, interface stiffness is modified by a parameter β_{ij} (Eq. 9) defined as the ratio between a geometric characteristic of actual masonry texture a_{ij}, namely block height or width, with respect to the overall distance d_{ij} between the connected elements, evaluated along the orthogonal direction with respect to the interface plane:

$$\beta_{ij} = a_{ij} / d_{ij} \quad (12)$$

In this manner, the model turns out to be less dependent on the coarse or fine façade discretisation adopted for the specific case study and, furthermore, it can still be used if the actual masonry texture needs to be considered, since β_{ij} becomes close to 1.

Assembling interface matrices in terms of element displacements **q** by means of compatibility matrices **H** (Eq. 5), the stiffness matrix **K** of the whole façade is obtained and the problem of a façade subjected to external forces $\mathbf{F}^{ext}$ may be statically solved [20]:

$$\mathbf{K}\,\mathbf{q} = \mathbf{F}^{ext} \quad (13)$$

2.3 Dynamic and modal analysis

The dynamic equilibrium of an assemblage of rigid elements can be formulated by expressing the equilibrium of the effective forces associated with each of its degrees of freedom. Then, a multi-degree-of-freedom (MDOF) equilibrium equation is obtained [20], [21]:

$$\mathbf{M}\,(\partial^2\mathbf{q}/\partial t^2) + \mathbf{K}\mathbf{q} = \mathbf{F}^{ext} \quad (14)$$

Where **M** is the mass matrix of the façade, collecting mass and polar inertia with respect to the coordinate system axis for each rigid element. Damping is neglected for simplicity. It is worth mentioning that setting $\mathbf{F}^{ext} = 0$, a standard eigenvalue problem is obtained:

$$\det[\mathbf{K} - \eta^2\mathbf{M}] = 0 \quad (15)$$

and the natural frequencies of the façade may be determined, together with the corresponding modal shapes and mass participation factors:

3 Numerical tests

3.1 Simple masonry façade with openings

The proposed approach is initially applied to a simple case study represented by a masonry façade taken from a generic two-storey building, with four equal openings placed symmetrically with respect to both plane directions (Figure 5). The geometry of this case study is taken from [22], where in-plane collapse load multipliers were determined by adopting a limit analysis approach. The façade is initially considered composed of blocks following a running bond arrangement as in the original contribution. Then, the façade is subdivided into rigid elements larger than single blocks, in order to evaluate the variations in terms of natural frequencies and corresponding modal shapes. Façade uniform thickness equal to 0.25 m, masonry density equal to 1800 kg/m^3, normal and shear stiffness equal to 10^6 kN/m and 4.17×10^5 kN/m, respectively, are assumed for determining natural frequencies. Façade displacements and rotations are fixed along its base, in order to allow simple out-of-plane vibration modes.

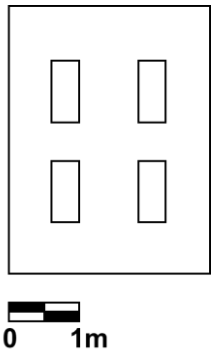


Fig. 5: Two-storey masonry façade with openings taken from [22]

Source: created by the author.

Modal analysis results limited to the first two frequencies are shown in Figure 6 for the detailed rigid model composed of regular blocks, whereas Figure 7 and Figure 8 present the same results for the rigid element model with quite large and large elements, respectively. In particular, a total of 68 elements in the first case and only 21 in the second

one are adopted, with respect to 146 blocks of the original case study.

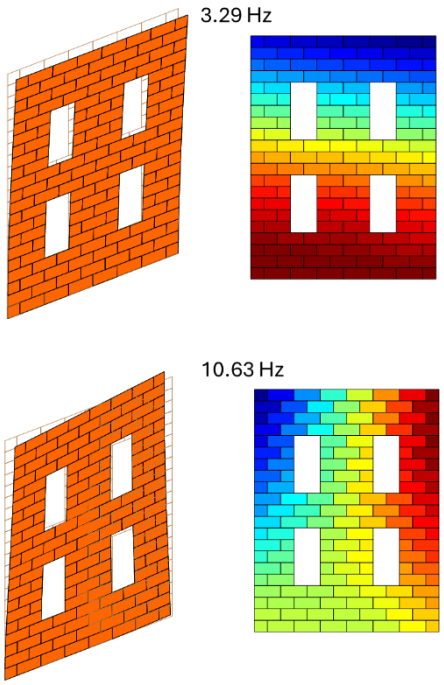


Fig. 6: First and second natural frequencies and modal shapes of the façade taken from [22] made of rigid blocks
Source: created by the author.

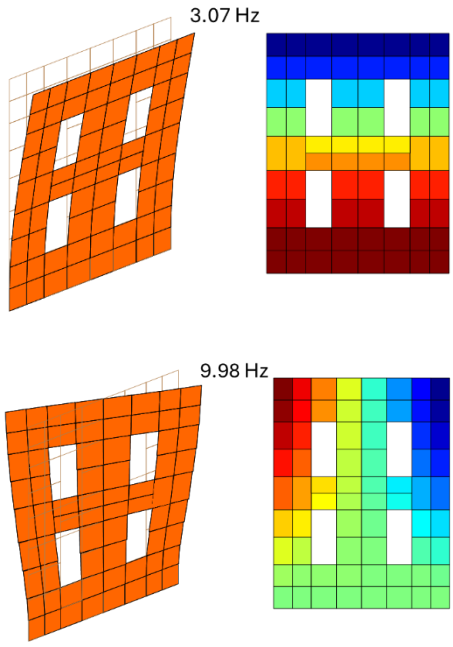


Fig. 7: First and second natural frequencies and modal shapes of the façade taken from [22] made of quite large rigid elements
Source: created by the author.

Modal shapes obtained with the three different façade discretisation types turn out to be in good agreement. As can be expected, the first modal shape is a simple out-of-plane bending deformation, whereas the second one is a torsional deformation with respect to the façade vertical axis of symmetry.

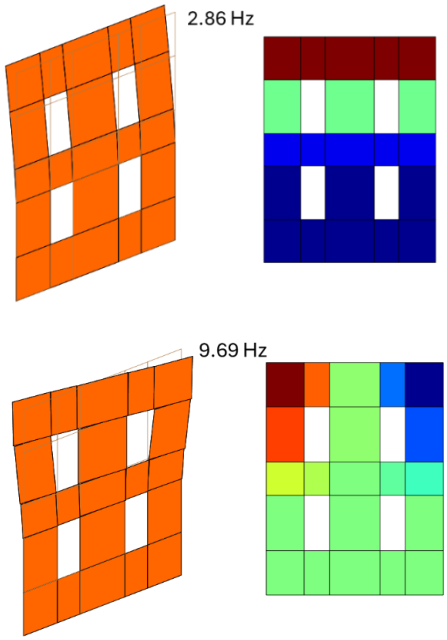


Fig. 8: First and second natural frequencies and modal shapes of the façade taken from [22] made of large rigid elements
Source: created by the author.

Furthermore, results in terms of natural frequencies turn out to be in quite good agreement, with differences close to 6% in the case of quite large elements (7% and 6% for the first and second frequencies/modal shapes, respectively), whereas differences are close to 10% (13% and 9% for the first and second frequencies/modal shapes, respectively) in the case of large elements. As expected, the model with large rigid elements turns out to be more rigid than that with regularly arranged blocks and convergence to the results of the original case study is found for increasing the number of overall rigid elements.

3.2 Façade in a building aggregate

The proposed approach is then applied to a specific case study that was subjected to on-site monitoring activities several years ago [23]. The macro-volume of the Western Museum of Lucania and the House of the Priore of the 'Certosa di San Lorenzo' located in Padula (Salerno), Italy (Figure 9 and Figure 10), were surveyed, considering them as a structurally homogeneous area, composed of several buildings generating an aggregate. The buildings belong to the same period of construction.

3.2.1 On-site dynamic structural identification

Surveying details can be found in [23]. Results of the monitoring campaign showed that the first mode of

vibration (frequency 1.86 Hz and damping coefficient 1.51%) involved the western façade, which could be considered the most vulnerable part of the building. This part is characterised by two internal floors and a basement; it has an irregular thickness along its height, and it is characterised by a limited number of orthogonal stiffening masonry walls. Then, the façade turns out to be slender and vulnerable to out-of-plane flexural mechanisms, and it turns out to be suitable for being modelled with the proposed rigid element approach.

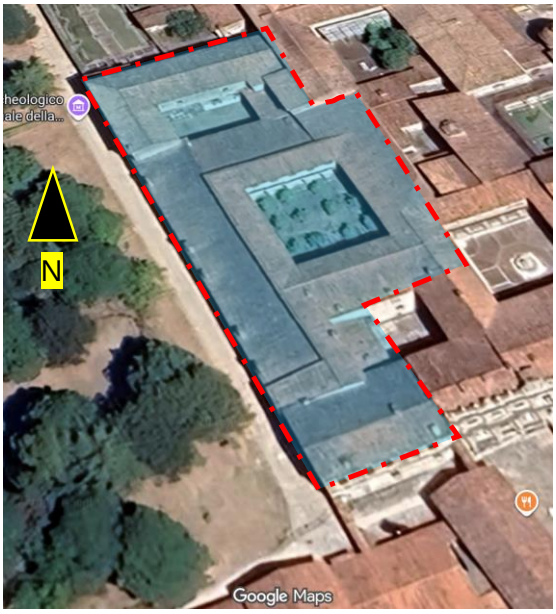


Fig. 9: Satellite view of the western portion of Certosa di San Lorenzo in Padula
Source: Google Maps and modified by the author.

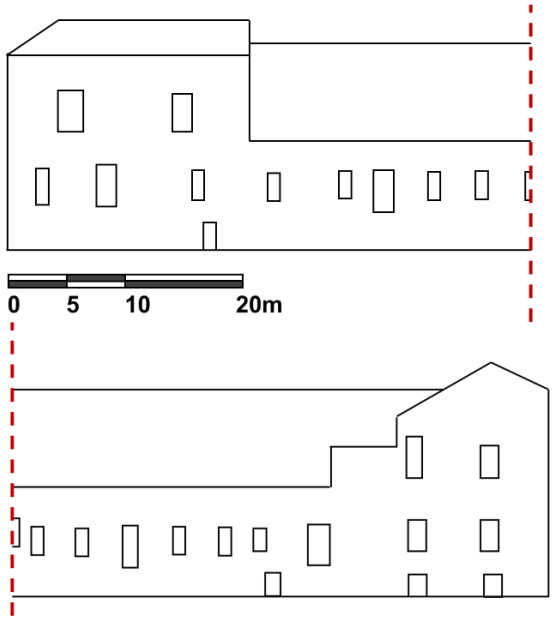


Fig. 10: Schematic view of the western façade of the western portion of Certosa di San Lorenzo in Padula and base section of the walls

Source: created by the author with reference to [23].

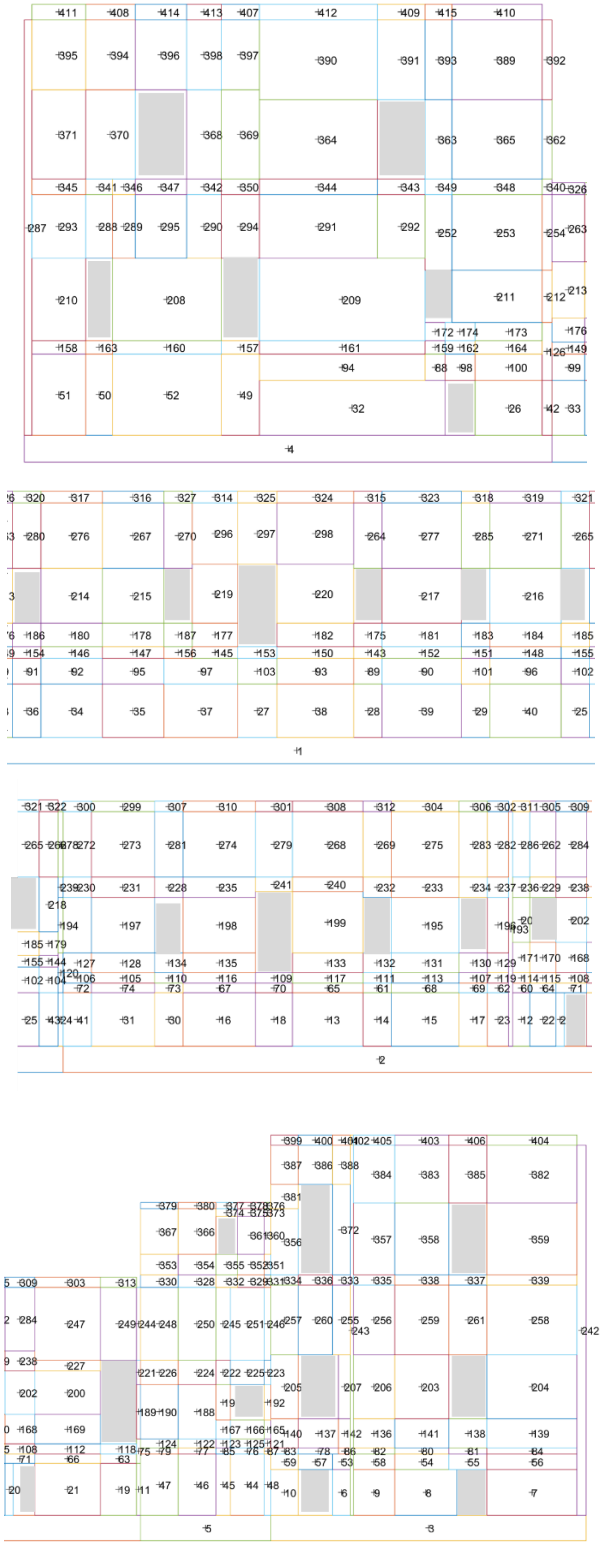


Fig. 11: Façade discretisation into rigid elements
Source: created by the author.

Then, specific dynamic identification on-site tests involved only the western façade, obtaining a first vibration mode in good agreement with previous surveying activities (frequency 1.98 Hz), mainly

involving the left-central portion of the façade at mid-height. The second vibration mode (frequency 2.40 Hz) involved more generally the upper floors of the façade and its central portion in the horizontal direction.

3.2.2 Numerical model and modal analysis

The rigid element model of the façade is generated by subdividing it into rectangular portions following the main façade openings, slab and roof levels, and building variations along height. In particular, thin vertical rectangular elements are defined between the façades of adjacent sub-buildings, whereas thin horizontal rectangular elements are defined at the base and at slab and roof levels. In this manner, additional rigid or elastic restraints are applied to account for the stiffening effect of foundations, orthogonal walls, and horizontal slabs and roofs. An overall number of 415 rigid elements is generated (Figure 11). An average façade thickness value equal to 1 m is assumed, together with masonry façade density equal to 1800 kg/m^3. Interface generic normal and shear stiffness parameters are assumed equal to 10^6 kN/m and 4.17×10^5 kN/m, respectively. Then, specific stiffness parameters are calculated as a function of the relative distance between each couple of adjacent rigid elements (Eq. 9). Numerical modal analysis is then performed, and among the results, the first and second frequencies are taken into consideration. Results obtained with the proposed rigid element model of the façade turn out to be in very good agreement with experimental results coming from the dynamic structural identification campaign, both in terms of frequencies and modal shapes (Figure 12). In particular, the differences between frequencies are less than 1% for the first one and less than 5% for the second one.

Table 1 collects details of frequencies determined from on-site dynamic identification tests, or Structural Health Monitoring (SHM) activities, together with numerical results obtained with a 3D Finite Element Model (FEM) of the building portion, with masonry walls modelled as quadrilateral shell elements [23], and with the results obtained with the proposed Rigid Element Model. The proposed model turns out to be more effective in matching on-site test results than the standard FEM adopted in [23]

Table 1. First and second natural frequencies of the façade of the 'Certosa di San Lorenzo' in Padula obtained with on-site tests and numerical models

	Natural frequencies [Hz]		
Mode	SHM [23]	FEM [23]	Rigid Element Model
1	1.98	2.60	1.97
2	2.40	3.02	2.50

Source: created by the author

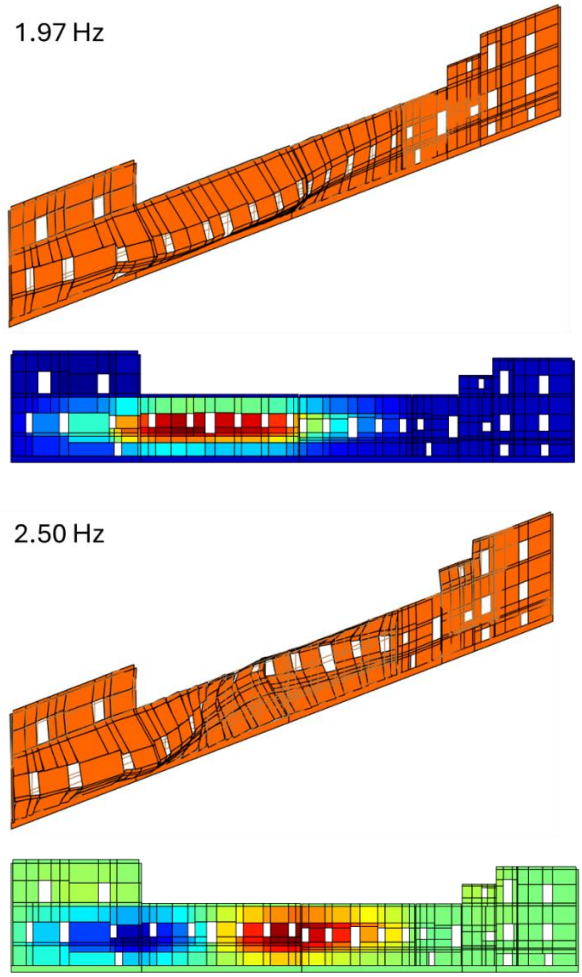


Fig. 12: First and second natural frequencies of the façade modelled with rigid elements, together with the corresponding modal shapes shown in 3D and by means of maps of out-of-plane displacements
Source: created by the author.

4 Conclusion

In this short contribution, an existing discrete/rigid block/element model, originally introduced for simulating the in-and out-of-plane behaviour of masonry walls with regular texture, was successfully extended to more generic case studies of masonry building façades subjected to out-of-plane actions. In detail, the original model was updated, allowing to account for a more generic discretisation of masonry walls or façades, by subdividing them into quadrilateral (square or rectangular) elements whose

size does not depend on single masonry block dimensions, but is more related to façade and building characteristics (openings, floor levels, orthogonal walls). A simple algorithm for element and interface determination was also proposed in order to allow the use of geometric information from standard DXF files.

The model effectiveness was evaluated by performing two numerical tests. The first one focused on a small masonry façade with openings, whereas the second one took into consideration an existing building façade. In the first case, the proposed models with quite large and large rigid elements turned out to be in agreement with the numerical model with small blocks following a regular texture, and a convergence to the behaviour of the original case study was found. In the second case, thanks to a good calibration of interface properties and model boundary conditions, the proposed model with large rigid elements turned out to be in good agreement with experimental data coming from a structural dynamic identification campaign.

Future developments of this work will focus on other real case studies, such as the second one considered here, by simulating the dynamic behaviour of façades taken from aggregate buildings typical of Italian town centres, by calibrating numerical model properties with respect to structural dynamic identification tests. Furthermore, the proposed model will also be adopted for performing in- and out-of-plane pushover analysis of the façades, to determine potential collapse loads.

Declaration of Generative AI and AI-assisted Technologies in the Writing Process

During the preparation of this work, the author(s) utilized artificial intelligence (AI) technologies solely for the purpose of linguistic refinement and grammatical correction. Following the application of these tools, the author(s) comprehensively reviewed, verified, and edited the resulting text. The author(s) maintain full accountability and responsibility for the accuracy, integrity, and final content of the publication.

References:

[1] Decanini, L., De Sortis, A, Goretti, A, Langenbach, R., Mollaioli, F, Rasulo, A., Performance of Masonry Buildings During the 2002 Molise, Italy, Earthquake, Earthquake Spectra, Vol.20, No.15, 2004, pp. 191-220. https://doi.org/10.1193/1.1765106

[2] Carocci, C.F., Small centres damaged by 2009 L'Aquila earthquake: on site analyses of historical masonry aggregates, Bulletin of Earthquake Engineering, Vol.10, 2012, pp. 45–71. https://doi.org/10.1007/s10518-011-9284-0

[3] Augenti, N., Parisi, F., Learning from Construction Failures due to the 2009 L'Aquila, Italy, Earthquake, Journal of Performance of Constructed Facilities, Vol.24, No.6, 2010, pp. 536-555. https://doi.org/10.1061/(ASCE)CF.1943-5509.0000122

[4] Penna, A., Morandi, P., Rota, M. et al. Performance of masonry buildings during the Emilia 2012 earthquake. Bulletin of Earthquake Engineering, Vol.12, 2014, pp. 2255–2273. https://doi.org/10.1007/s10518-013-9496-6

[5] Sorrentino, L., Cattari, S., da Porto, F. et al. Seismic behaviour of ordinary masonry buildings during the 2016 central Italy earthquakes. Bulletin of Earthquake Engineering, Vol.17, 2019, pp. 5583-5607. https://doi.org/10.1007/s10518-018-0370-4

[6] D'Ayala, D.-Speranza, E., Definition of Collapse Mechanisms and Seismic Vulnerability of Historic Masonry Buildings, Earthquake Spectra, Vol.19, No.3, 2003, pp. 479-509. https://doi.org/10.1193/1.1599896

[7] Modena, C., Valluzzi, M.R., Binda, L., Cardani, G., Saisi, A., Vulnerability of Historical Centres in Seismic Area Reliability of Assessment Methods for Different Building Typologies, 13th International Brick and Block Masonry Conference, Amsterdam, Netherlands, July 4-7, 2004, pp. 1-10.

[8] Binda, L; Cardani, G; Saisi, A; Valluzzi, M.R., Vulnerability analysis of the historical buildings in seismic area by a multilevel approach, Asian Journal of Civil Engineering, Vol.7, No.4, 2006, pp. 343-357.

[9] Formisano, A., Florio, G., Landolfo, R., Mazzolani, F.M, Numerical calibration of an easy method for seismic behaviour assessment on large scale of masonry building aggregates, Advances in Engineering Software, Vol.80, 2015, pp. 116-138. https://doi.org/10.1016/j.advengsoft.2014.09.013

[10] Angiolilli, M., Lagomarsino, S., Cattari, S., Degli Abbati, S., Seismic fragility assessment of existing masonry buildings in aggregate, Engineering Structures, Vol.247, No.113218, 2021. https://doi.org/10.1016/j.engstruct.2021.113218

[11] Degli Abbati, S., D'Altri, A.M., Ottonelli, D., Castellazzi, G., Cattari, S., de Miranda, S., Lagomarsino, S., Seismic assessment of interacting structural units in complex historic masonry constructions by nonlinear static analyses, Computers & Structures, Vol.213, 2019, pp. 51-71. https://doi.org/10.1016/j.compstruc.2018.12.001.

[12] Valente, M., Milani, G., Grande, E., Formisano, A., Historical masonry building aggregates: advanced numerical insight for an effective seismic assessment on two row housing compounds, Engineering Structures, Vol.190, 2019, pp. 360-379. https://doi.org/10.1016/j.engstruct.2019.04.025

[13] Grillanda, N., Valente, M., Milani, G., Chiozzi, A., Tralli, A., Advanced numerical strategies for seismic assessment of historical masonry aggregates, Engineering Structures, Vol.212, no.110441, 2020. https://doi.org/10.1016/j.engstruct.2020.110441

[14] Casolo S., Modelling the out-of-plane seismic behaviour of masonry walls by rigid elements, Earthquake Engineering and Structural Dynamics, Vol.29, 2000, pp.1797-1813. https://doi.org/10.1002/1096-9845(200012)29:12<1797::AID-EQE987>3.0.CO;2-D

[15] Cennamo, C., Chiaia, B.M., D'Angelo, S., Ferretti, D., Seismic Assessment and Rehabilitation of a Historical Theater Based on a Macro-Element Strategy, International Journal of Architectural Heritage, Vol.5, no.3, 2011, pp. 264-295. https://doi.org/10.1080/15583050903560256

[16] Vaculik, J., Griffith, M. Magenes, G., Dry Stone Masonry Walls in Bending-Part II: Analysis. International Journal of Architectural Heritage, Vol.8, no.1, 2014, pp. 29-48. https://doi.org/10.1080/15583058.2012.663060

[17] Smoljanović, H., Živaljić, N., Nikolić, Ž., A combined finite-discrete element analysis of dry stone masonry structures, Engineering Structures, Vol.52, 2013, pp. 89-100. https://doi.org/10.1016/j.engstruct.2013.02.010

[18] Ferreira, T.M., Costa, A.A., Costa, A., Analysis of the out-of-plane seismic behavior of unreinforced masonry: a literature review, International Journal of Architectural Heritage, Vol.9, No.8, 2015, pp. 949-9772. http://dx.doi.org/10.1080/15583058.2014.885996

[19] Cecchi, A., Sab, K., A comparison between a 3D discrete model and two homogenised plate models for periodic elastic brickwork, International Journal of Solids and Structures, Vol.41, No.9-10, 2004, pp. 2259-2276. https://doi.org/10.1016/j.ijsolstr.2003.12.020

[20] Baraldi, D., Cecchi, A., Discrete and continuous models for static and modal analysis of out of plane loaded masonry, Computers and Structures, No.207, 2018, pp.171-186. https://doi.org/10.1016/j.compstruc.2017.03.015

[21] Baraldi, D., Reccia, E., Cecchi, A., Discrete model for out-of-plane loaded random masonry, ECCOMAS Procedia, COMPDYN 2017, Rhodes Island, Greece, 15-17 June, 2017, pp. 2505-2518. https://doi.org/10.7712/120117.5584.17916

[22] Ferris, M.C., Tin-Loi, F., Limit analysis of frictional block assemblies as a mathematical program with complementarity constraints, International Journal of Mechanical Sciences, Vol.43, no.1, 2001, pp. 209-224. https://doi.org/10.1016/S0020-7403(99)00111-3

[23] Aldreghetti, I., Boscato, G., Fiorin, M., Massaria, L., Scafuri, V., Simplified procedure for structural integrity evaluation of complex walls through signal energy analysis based on vibrational data, WIT Transactions on The Built Environment, Vol.203, 2021, pp. 133-145. https://doi.org/10.2495/STR210121

[24] Lemos, J.V., Discrete Element Modeling of Masonry Structures, International Journal of Architectural Heritage, Vol.1, no.2, 2007, pp. 190–213. https://doi.org/10.1080/15583050601176868

Contribution of Individual Authors to the Creation of a Scientific Article (Ghostwriting Policy)

The author contributed in the present research, at all stages from the formulation of the problem to the final findings and solution.

Source of Funding for Research Presented in a Scientific Article or Scientific Article Itself

The work was partly financed by the National Recovery and Resilience Plan (NRRP), Mission 4, Component 2, Investment 1.1, Call for tender No. 1049 published on 14.9.2022 by the Italian Ministry of University and Research (MUR), funded by the European Union - Next-GenerationEU - Project Title 'Multiscale and mUltidisciplinaRy Approach for hisTOrical centres ResIlience (MURATORI)' - CUP: F53D2300954001, project code P2022339JP, 'PRJ-0257' - Grant Assignment Decree No. 12072023 adopted on 28.07.2023 by the Italian Ministry of University and Research (MUR).

Sources of Funding for Research Presented in a Scientific Article or Scientific Article Itself

No funding was received for conducting this study.

Conflict of Interest

The author has no conflicts of interest to declare that are relevant to the content of this article.

Creative Commons Attribution License 4.0 (Attribution 4.0 International, CC BY 4.0)

This article is published under the terms of the Creative Commons Attribution License 4.0
https://creativecommons.org/licenses/by/4.0/deed.en_US